Ghost Image Due to mmWave Radar Interference: Experiment, Mitigation and Leverage

Yawen Fan, Jingchao Bao, Kai Wu and Husheng Li

***Abstract*—Millimeter wave (mmWave) radar is becoming a major instrument for the ranging, Doppler and imaging of environment in various applications such as autonomous driving and unmanned aerial vehicles. As substantially more radar devices are employed in applications, the interference among different radar transceivers becomes a severe problem, which may bring substantial damages to the applications of radar. One of these impacts is the ghost image caused by the interference, which results in a fake object. In this paper, experiments are carried out to demonstrate the existence of ghost image, based on 77GHz mmWave automobile radar. Detailed analysis is carried out based on the experimental measurements for disclosing the mechanism of interference and the properties of the corresponding ghost image. The prominent features of ghost image include statistically narrow frequency spread, abnormal Doppler estimation and possible negative distance. Based on the these features, systematic approaches are introduced to mitigate the interference induced ghost images. Meanwhile, schemes are proposed to leverage the ghost images for locationing and communications, instead of merely removing them.**

I. Introduction

Radar technology, as a powerful tool to sense the environment, has found many applications in modern cyber physical systems (CPSs), such as unmanned aerial vehicular (UAV) networks and autonomous vehicle networks. In these systems, each node uses radar to monitor the positions and speeds of neighboring nodes, for the avoidance of collision or formation control. Different from wireless data communications, in which interference is a major concern, there have been very few studies on the mutual interference of radar signals. On one hand, it is because traditional radar systems are often employed in an isolated manner. On the other hand, radar systems, such as the frequency-modulation continuous-wave (FMCW) systems, are robust to interference; even if some sporadic interference is received by radar receivers, it can be eliminated by the inherent capability of interference mitigation in the radar receiver (e.g., being removed by Kalman filtering). However, in the new applications in which there are unprecedentedly many radar transceivers (e.g., there could be hundreds of radars within hundreds of meters for UAV networks), the interference could be very dense and may be beyond the traditional interference-proof capability of radar systems. If the interference incurs estimation errors on positions and speeds, it could be detrimental to the corresponding systems, e.g., collisions of vehicles or the loss of UAV formations.

Y. Fan and J. Bao were, and H. LI is, with the Department of Electrical Engineering and Computer Science, The University of Tennessee, Knoxville, TN (emails: yfan12,jbao2,hli31@utk.edu). Currently Fan and Bao are working in Zoox Inc. and Qualcomm Inc., respectively. K. Wu is with University of Technology Sydney, Australia (email: kai.wu@uts.edu.au).

In this paper, we focus on the millimeter wave (mmWave) FMCW radar and carry out experiment using 77GHz radar to demonstrate the ghost image due to interference. From experimental measurements, we will analyze the prominent features of ghost images for distinguishing it from real reflecting objects. Based on these features, we will propose a systematic approach to detect and eliminate the ghost images. Different from existing studies that all endeavor to remove the interference, we will propose schemes to leverage the interfering signal to infer information on the interferer, as well as endowing the interferer the capability of joint radar and communications.

The remainder of this paper is organized as follows. The background on mmWave FMCW radar and the related work are introduced in Section II. The experiment is introduced in Section III, which also analyzes the features of ghost images. The mitigation and leverage of ghost images are discussed in Sections IV and V, respectively. Finally the conclusions are drawn in Section VI.

II. Background and Related Work

In this section, we introduce the background of mmWave FMCW radar and the corresponding related work on radar interference.

A. Principle of FMCW Radar

1) Radar Signal Model: In this paper, we consider FMCW radar systems, whose processing procedure is illustrated in Fig. 1. The radar transmitter sends out chirps with period T_p. The pulse sent by the radar transmitter is given by

$$f(t) = A\exp\left(j\left(2\pi(f_0+0.5St)t+\phi\right)\right), \qquad t\in[0,T_c], \quad (1)$$

where A is the amplitude, f_0 is the starting frequency, S is the frequency increasing slope, ϕ is the phase, and T_c is the chirp duration. It is required $T_c < T_p$. When the distance between the transmitter and reflecting object is d, the round trip time (also the delay of received signal) is $\tau_d = \frac{2d}{c}$, where c is the light speed.

2) Ranging: At the radar receiver, the received signal is mixed with the local oscillation. The output signal is given by

$$f_o(t) \quad = \quad \eta A\exp(j(2\pi S\tau_d t+\phi')), \qquad (2)$$

where η is the amplitude degradation of the received signal, and the phase ϕ' is given by $\phi' = f_0\tau_d - 0.5S\tau_d^2$. The frequency of $S\tau_d$ is called the beat frequency and is denoted by f_b. When the estimation on the beat frequency is $\hat{f}_b$, which is obtained from DFT on the samples of mixer output, the

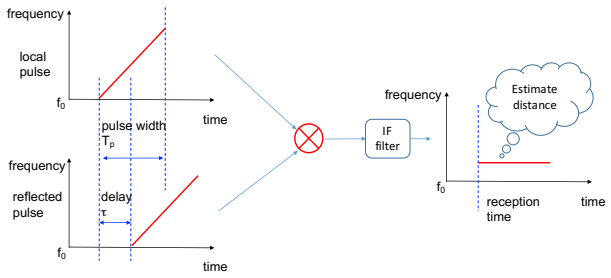

Fig. 1: An illustration of FMCW signal processing procedure

TABLE I: Existing Works on Radar Interference

Items	FMCW Radar	Pulsed Radar
PHY	Signal clip or notch filter [4], independence component separation [20], interference cancellation [3], Interference detection [14], Interpolation [15], noise cancellation [8], Deep learning [13]	Anti-jamming [4]
MAC	Frequency hopping [11], Coordination [2], chirp sequence [19], orthogonal sequence [18], Avoidance [17]	Separation from comm. [10]
Damage Analysis	Ghost target [7], [9]	Increased noise and ghost target [6]

estimation of the range is given by $\frac{\hat{f}_b c}{2S}$. The distance resolution is given by $\frac{c}{B}$, where $B = ST_c$ is the bandwidth scanned by each chirp [1].

3) Doppler: Different from other radar systems using the Doppler effect to estimate the object speed, the mmWave FMCW radar leverages the sensitivity of signal phase to the object movement (which is essentially equivalent to the Doppler effect). It is shown in [1] that the estimation of object speed is given by

$$\hat{v} = \frac{\lambda \delta\theta}{4\pi T_c}, \tag{3}$$

where λ is the wave length, and $\delta\theta$ is the phase change at the peak frequencies of two successive chirps.

B. Related Work

In [12], seven scenarios of radar interference and nine possible solutions have been discussed. The corresponding feasibility has been analyzed with either experimental results or simulations. Although the report claims that radar interference in typical road scenarios is 'unlikely to cause harmful malfunction', this conclusion obtained in 2012 may no longer be valid in the future when much more radar systems are put into use. A more recent report on the same issue is given in [16], which summarized the interference of radar in different scenarios. More related work is summarized in Fig. I.

III. Experiment and Analysis

In this section, we introduce our experiment results and carry out analysis on the measurement, which provides hints to the mitigation and leverage of the radar interference.

Parameter	Value
Start Frequency (GHz)	77
Freq. Slope (MHz/us)	29.982
Samples per Chirp	256
Chirp Duration (us)	60
Idle Time (us)	100

Fig. 2: Parameters of the experiment

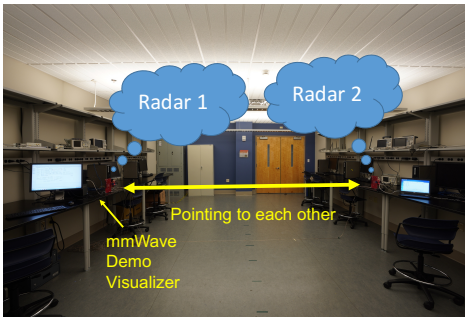

Fig. 3: Experiment setup

A. Experiment

We use two mmWave radars (TIAWR1243/1642) in the 77GHz band. The corresponding parameters are given in Fig. 2. Each radar is equipped with an AWR1642Boost evaluation board. The corresponding setups of radar are summarized in Fig. 2. We place the two radar antennas pointing to each other, as shown in Fig. 3. A key challenge is to synchronize the chirps at the two radars, in order to accelerate the experiment. The hardware trigger for synchronization is initiated by a square wave from an Arduino zero board, which is wired to both radar transceivers, with a period of 51ms (15ms high +36ms low).

The experiment result is shown in Fig. 4, where the display interface of the Demo Visualizer is shown. The horizontal and vertical axes are the Doppler (velocity) and range (distance) of the detected object, respectively. The left figure displays the detected object without interference, which shows a static object (actually the other radar antenna, table and wall) at the distance of around 10 meters. However, when there exists interference between the radars, the right figures shows an extra horizontal bar, which indicates an object moving with a speed between 0 and 10 meters per second at the opposite direction. Obviously, this ghost image stems from the interference of the other radar. This demonstrates the potential damage to radar systems due to interference.

B. Analysis

We recorded the samples at the interfered receiver with 256 samples per chirp. For each setup, we use 400 chirps for the analysis. Before we analyze the ranging and Doppler results due to interference, we provide a mathematical model for the impact of interference first.

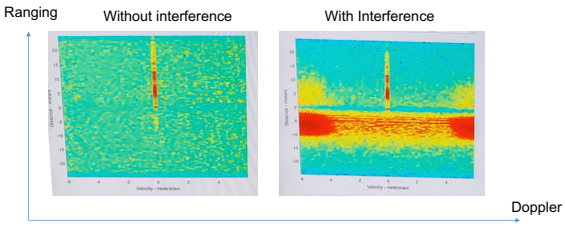

Fig. 4: Experiment result display

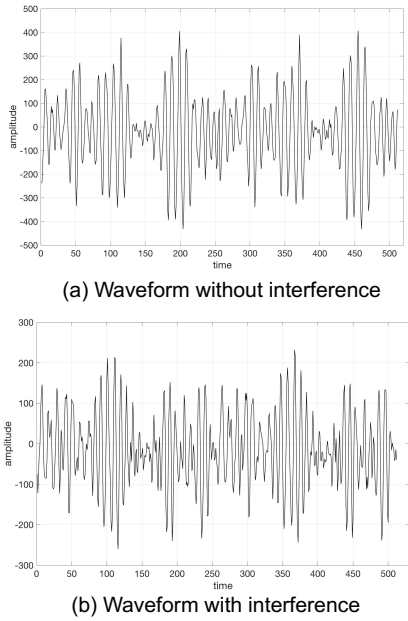

Fig. 5: Waveforms with and without interference

1) Impact of Interference: We assume that the received interference signal within a chirp period is given by

$$f^I(t) = A_0 \exp\left(j\left(2\pi\left(f_0 + \frac{1}{2}S(t-\tau_0)\right)(t-\tau_0) + \phi_I\right)\right), \quad (4)$$

where τ_0 is the sum of the interference signal travel time and the starting time difference and ϕ_I is the initial interference chirp phase. Then, the output of the mixer, generated by the interference, is given by

$$f_o^I(t) = A_0 \exp\left(j\left(2\pi S\tau_0 t + \phi'\right)\right), \quad (5)$$

where ϕ' is the phase difference, and the beat frequency is given by $f_b^I = S\tau_0$.

2) Ranging: The output waveforms of the mixture at the receiver with and without interference are depicted in Fig. 5, each consisting of about 2 chirps. It cannot be distinguished whether the receiver is interfered merely from the time-domain waveform. Moreover, the average signal power is also similar in both cases. Hence, traditional approaches using received power to detect the interference cannot be applied. Note that, in the ideal case (namely there is a single reflection path) the mixture output should be a single-tone sinusoid, whose frequency is determined by the round trip distance. However, the waveforms in Fig. 5 experience amplitude modulations.

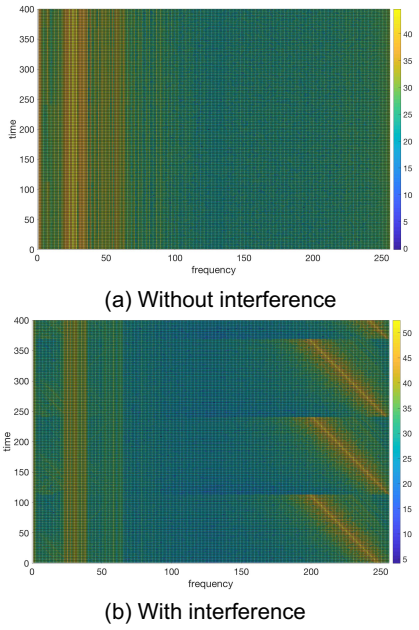

Fig. 6: Spectrograms with and without interference

It is due to the multiple paths of reflection (thus resulting in multiple traveling times and beat frequencies).

To exploit more features for distinguishing the interference, we plotted the spectrograms with and without interference in Fig. 6. The distinction between the cases with and without interference can be easily seen: in the right end of the DFT spectrum (the negative frequency band) there exists a significant frequency component whose frequency increases periodically. This extra frequency peak is due to the mixing of the receiver local oscillation and the interference. When there exists both real reflectors and interference, the mixer output is then given by

$$\begin{aligned} f_o(t) &= \sum_{k=1}^{K} A_k \exp(j\left(2\pi S\tau_k t + \phi_k\right)) \\ &+ A_0 \exp(j2\pi\left(S\tau_0 + \phi'\right)), \end{aligned} \quad (6)$$

where A_k, τ_k and ϕ_k, $k = 1, ..., K$, are the amplitudes, round trip times and phases for the k-th reflector. From Fig. 6, we observe that $K > 0$. Moreover, the periodic shift of the peak frequency of the interference is because that the interferer and receiver have different chirp starting times. In the experiment, due to the different arrival times of the triggering signal, the phase of the interferer is ahead of the receiver, thus endowing the mixer output negative frequency components (and therefore the negative distance).

To further demonstrate the above conclusion, we plotted the spectrums of the mixer outputs for a single chirp in Fig. 7. We observe a single peak in the interference side (the right hand end of the figure, or equivalently the negative frequency side). We also observe that the spectrum spread around the peak of the real reflected signal is significantly wider than that of the interference. This is because that the reflectors (tables, wall, desktop, et al in the experiment) result in substantially different

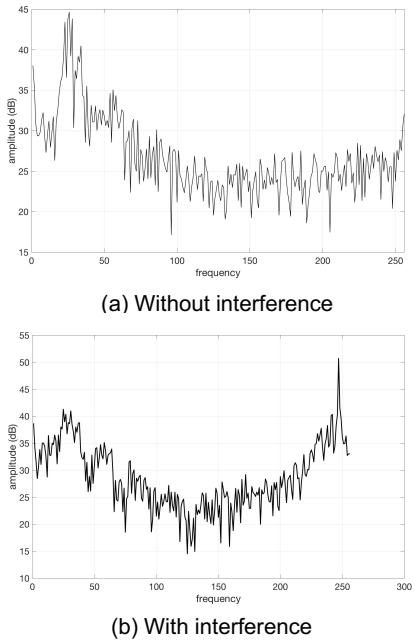

Fig. 7: Single-chirp spectrums with and without interference

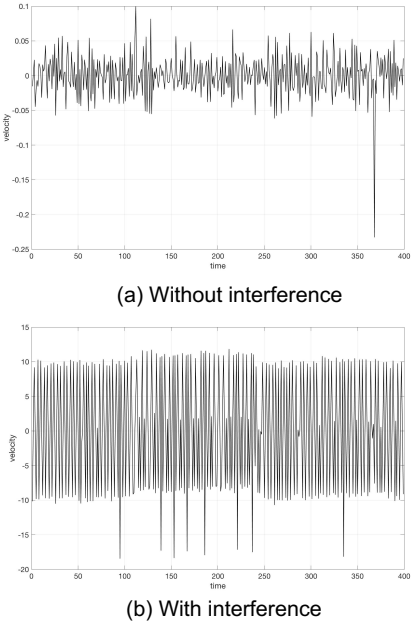

Fig. 8: Doppler estimations with and without interference

round trip times, which are converted to the frequency spread at the mixer output. The interference is from a single antenna, which is equivalent to an almost point reflector.

3) Doppler: We used the approach in Sec. II to calculate the Doppler (velocity) for the experimental measurement. The results are shown in Fig. 8. We observe that the estimated velocity of the non-interference case oscillates around 0 with small amplitudes (in the order of cm/s). In the experiment, the reflectors are stationary; the oscillation is caused by noise in the samples. In a sharp contrast, the estimated velocity in

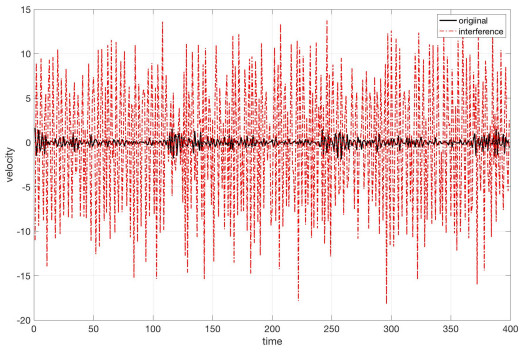

Fig. 9: Comparison between the Dopplers due to reflected signal and interference

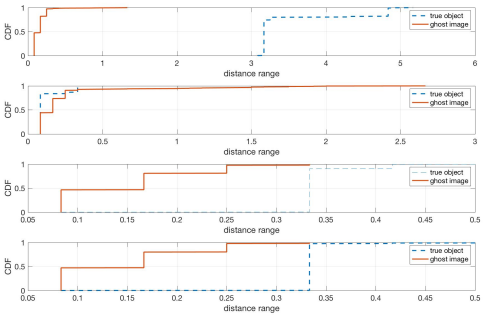

Fig. 10: CDFs of distance deviations in four experiments (solid: interference; dotted: without interference)

the case of interference is of much greater magnitude (tens of meters per second); moreover, it oscillates radically, which is obviously abnormal. The reason behind the large-magnitude oscillation in the velocity estimation is that the phase difference between the interferer and receiver is random across different chirps, which makes the velocity estimation based on the phase difference across successive chirps unreasonable.

IV. Mitigation of Interference

In this section, we discuss the approaches to mitigate the radar interference. In traditional approaches, the interference is usually detected by abnormally high signal strength. However, as we have demonstrated in the experiment, in the context of mmWave FMCW radar, the interference power is not necessarily greater than the reflected signal. Therefore, we propose to use the frequency spread, range abnormality, and Doppler abnormality to detect the interference and filter it out.

A. Frequency Spread

As discussed in Section III, the interference results in a narrow frequency spread in the spectrum of the mixer output, which indicates a 'reflector' with almost identical round trip time. On the other hand, in practice (e.g., on highways), the reflectors usually have a significant spatial spread, which results in different signal round trip times and significant frequency spread. We plotted in Fig. 10 the cumulative distribution

	frequency spread	range abnormality	Doppler abnormality
prominence	almost necessary but not sufficient	sufficient but not necessary	almost necessary and sufficient
pros	need only one chirp	strong sufficiency, need only one chirp	strong sufficiency
cons	may also happen to true reflectors	happens with probability 1/2	need multiple successive chirps

Fig. 11: Summary of properties of ghost image features

functions (CDFs) of frequency spreads of the true reflectors (dotted) and interferers (solid) in four different experimental setups. Here the frequency spread is defined as the 3-dB bandwidth around the spectrum power peak. It is observed that, except for the second experiment, the frequency spreads (spatial spreads) of true reflectors are statistically greater than those of interferer. In all these experiments, the ghost image generated by the interferer has narrow frequency spreads. In the second experiment, the reflector is the wall, which results in the narrow frequency spread. From these preliminary results, we conclude that the frequency spread is a significant, but not a decisive, indictor for the interference.

B. Range Abnormality

A more reliable feature, but not always present, is the abnormality in the range estimation. As we have observed in the experiment, when the phase of the interference signal is ahead of that of the interfered radar, the interference will result in negative frequency component at the output of the mixer. This negative frequency (thus negative distance) is unreasonable. Therefore, it is sure to determine the interference from the negative frequency component. However, it is possible that the interference signal phase is behind that of the interfered radar; therefore, the interference does not necessarily yield negative frequency components and the abnormality.

C. Doppler Abnormality

The most reliable feature is the Doppler abnormality. Since it is generated by the initial phase randomness of the interference signal, it results in unreasonable trajectories of velocity estimations (e.g., with plenty of radical oscillations). However, it requires multiple successive chirps of interference. A single chirp does not generate a velocity estimation; even two successive chirps may generate reasonable estimations (e.g., tens of meters per second, which is reasonable in highway traffics). Hence, this approach is invalid for sporadic interferences.

D. Mitigation Scheme

The properties of the above three features for distinguishing the ghost image due to interference are summarized in Fig. 11. Based on these features, we propose a procedure for mitigating the ghost images due to interference. In summary, we use the above three features to check different peaks in the frequency spectrum (namely different prominent reflectors)

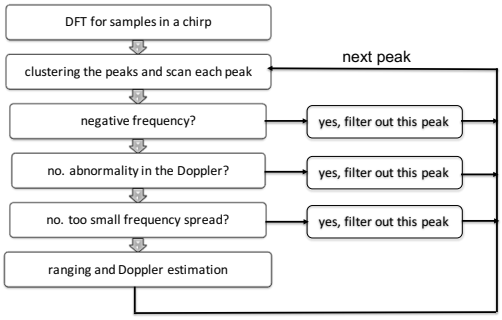

Fig. 12: Procedure of removing ghost images due to interference

and determine whether they are ghost images. Once a peak is determined to be a ghost image, it will be removed using a notch filter. The detailed procedure is summarized in Fig. 12. We have applied the proposed procedure to remove the ghost images in our experiment measurements. All ghost images are removed, while all real reflectors are kept.

V. Leveraging Ghost Images

In all existing studies on ghost images of radar interference. the purpose is to remove the ghost images using the corresponding features. In this section, we discuss how to leverage the ghost images to glean or convey information, since every signal in the environment could provide information.

A. Sensing

Once a peak in the frequency spectrum is determined to be a ghost image, the receiver can leverage it to retrieve information of the interferer. Besides knowing the existence of a radar transmitter, the interfered receiver can endeavor to glean the position information of the interferer. Due to the phase incoherency, it is impossible to determine the distance using the beat frequency. However, the position of the interferer can be estimated if the receiver is equipped with multiple antennas:

- If the interfered receiver has an antenna array (which is typical for modern mmWave automobile radars) at one position, the receiver can filter out legitimate signals from true reflectors and use the interfering signal to estimate the corresponding angle of arrival (AOA).
- If the interfered receiver has multiple antenna arrays with a significant distance (e.g., arrays at different locations of an automobile, or radars at different vehicles with communications), the estimated AOAs can be used to estimate the position of the interferer by extending the incident lines.

The above schemes require the overhead of sampling and storing the received signals at each receive antenna. If the signals from different antennas have been combined before the mixer, as it is in our experiment, the ghost image can no longer be used to infer the position information of the interferer.

B. Communications

From the viewpoint of the interferer, the interference can be used to broadcast information (e.g., the radar transmitter ID

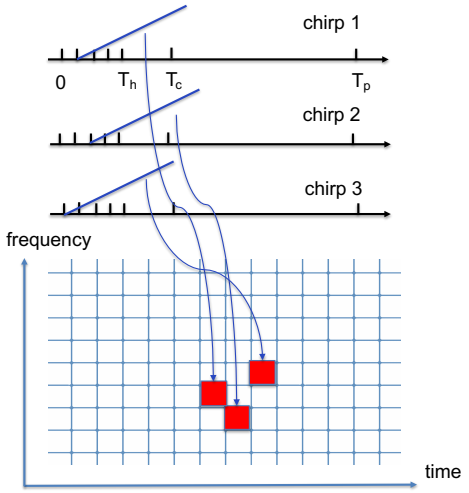

Fig. 13: An illustration of the PPM-like modulation scheme

or position) by modulating its radar signal[1]. Since there is no calibration between the interferer and interfered receiver, traditional coherent modulation schemes of PAM, PSK and FSK cannot be employed. However, as has been analyzed in Section III, the interference signal forms patterns in the spectrogram due to the varying timing in the chirps. This motivates us to propose a modulation scheme similar to the pulse position modulation (PPM), whose information modulated in the time will be converted to the beat frequency at the output of the mixer.

In more details, the radar transmitter defines an interval $[0, T_h] \subset [0, T_p]$, where T_h is the maximum chirp time delay. The interval is divided into N equal sub-intervals. At chirp k, the starting time within the chirp period is denoted by $\tau_k = \frac{j_k T_h}{N}$, where $j_k \in \{0, 1, ..., N-1\}$. Then, the starting time τ_k is converted to the beat frequency $f_k = S\left(\tau_k - \delta t - \frac{d}{c}\right)$, where d is the distance between the interferer and receiver and δt is the timing difference between the interferer and receiver. This procedure is illustrated in Fig. 13. Since there is no timing calibration between the interferer and receiver, the modulation should be differential, namely the information is modulated in the change of the chirp starting time.

Since the starting time of the interference chirp is obtained from the beat frequency, the time resolution, namely $\frac{T_h}{N}$ should make the beat frequency distinguishable. Since the distance resolution is given by $\frac{c}{ST_c}$ [1], the minimum $\frac{T_h}{N}$ should satisfy $\frac{T_h}{N} \geq \frac{1}{ST_c}$, which results in

$$N \leq \min\{ST_cT_h, T_cf_s\}, \tag{7}$$

where f_s is the sampling rate for the mixer output. The selection of T_h should assure that $S\left(T_h - \left(\delta t + \frac{d}{c}\right)\right) \leq \frac{f_s}{2}$, namely the mixer output with beat frequency should be losslessly sampled with frequency f_s. Using the parameters in the experiment and supposing $\delta t = 0$, $d = 100m$ and $T_cf_s = 256$, we have $T_h = 1.7us$ and $N \leq \min\{2520, 256\} = 256$, which implies that the every two successive chirps of the interference can convey approximately 8 bits, in the ideal case.

[1]Such a joint communication and radar scheme has been tested in experiment [5], using frequency increasing slopes.

VI. Conclusions

In this paper, we have introduced the experimental results of interference-induced ghost images based on 77GHz mmWave FMCW radar. The prominent features of the ghost images have been analyzed, based on which a systematic scheme of mitigating the ghost images has been proposed. Moreover, we have proposed to leverage the interference to infer the position of the interferer, as well as to broadcast information by the interferer.

References

[1] S. Rao, *Introduction to mmwave Sensing: FMCW Radars*, Texas Instruments Technical Report, 2018.

[2] C. Aydogdu, N. Garcia, L. Hammarstrand, H. Wymeersch, "Radar communication for combating mutual interference of FMCW radars," in *Proc. of IEEE Radar Conference*, 2019.

[3] J. Bechter and C. Waldschmidt, "Automotive radar interference mitigation by reconstruction and cancellation of interference component," in *Proc. of IEEE International Conference on Microwave for Intelligence Mobility*, 2015.

[4] G. M. Brooker, "Mutual interference of millimeter wave radar systems," *IEEE Trans. on Electromagnetism Compatibility*, vol. 49, no.1, pp.170–181, Feb 2007.

[5] Y. Fan, J. Bao, M. S. L. Aljumaily and H. Li, Communications via frequency-modulated continuous-wave radar in millimeter wave band," in *Proc. of IEEE Global Communications Conference*, 2019.

[6] M. Goppelt, H. L. Blocher and W. Menzel, "Automotive radar - investigation of mutual interference mechanisms," *Advances in Radio Science*, vol.8, pp.55-60, 2010.

[7] M. Goppelt, H. L. Blocher and W. Menzel, "Analytical investigation of mutual interference between automotive FMCW radar sensors," in *Proc. of the 6th German Microwave Conference*, 2011.

[8] F. Jin and S. Cao, "Automotive radar interference mitigation using adaptive noise canceller," *IEEE Trans. on Vehicular Technology*, vol. 67, no.4, April 2019.

[9] G. Kim, J. Mun, J. Lee, "A peer-to-peer interference analysis for automotive chirp sequence radars," *IEEE Trans. on Vehicular Technology*, vol. 67, no.9, Sept. 2019.

[10] Y. Li, L. Zheng, M. Lops and X. Wang, "Interference removal for radar/communication co-existence: The random scattering case," *IEEE Trans. on Wireless Communications*, vol.18, no.10, pp.4831-4845, Oct. 2019.

[11] T. N. Luo, C. E. Wu, Y. E. Chen, "77-GHz CMOS automotive radar transceiver with anti-interference function," *IEEE Trans. on Circuits and Systems-1. Regular Papers*, vol.60, no.12, pp.3247-, 3255, Dec. 2013.

[12] European Commission, *More Safty for All by Radar Interference Mitigation,* Technical Report, 2012.

[13] J. Mun, H. Kim and J. Lee, "A deep learning approach for automotive radar interference mitigation," arxiv, 2019.

[14] S. Murali, K. Subburaj, B. Ginsburg and K. Ramasubramanian, "Interference detection in FMCW radar using a complex baseband oversampled receiver," in *Proc. of IEEE Radar Conference*, 2018.

[15] S. Neemat, O. Krasnov and A. Yarovoy, "An interference mitigation technique for FMCW radar using beat-frequencies interpolation in the STFT domain," *IEEE Trans. on Microwave Theory and Technology*, vol. 67, no. 3, March 2019.

[16] National Highway Traffic Safety Administration, *Radar Congestion Study*, Technical Report, 2018.

[17] S. Sanka, *Radar to Radar Interference for 77GHz Automotive Radars*, Master Thesis, Delft University of Technology, 2017.

[18] S. Skaria, A. Al-Hourani, R. J. Evans, K. Sithamparanathan and L. Parampalli, "Interference mitigation in automative radars using pseudo-random cyclic orthogonal sequences," *Sensors*, vol. 19, 2019.

[19] Y. S. Son, H. K. Sung and S. W. Heo, "Automotive frequency modulated continuous wave radar interference reduction using per-vehicle chirp sequences," *Sensors*, vol. 18, 2018.

[20] F. Uysal and S. Sanka, "Mitigation of automotive radar interference," in *Proc. of IEEE Radar Conference*, 2018.